OMICS A Journal of Integrative Biology
Volume 20, Number 11, 2016

DOI: 10.1089/omi.2016.0112

Research Article

Cerebrospinal Fluid Metabolomics After Natural Product Treatment in an Experimental Model of Cerebral Ischemia

Tao Huan,[1,*] Jia Wen Xian,[2,*] Wing Nang Leung,[2] Liang Li,[1] and Chun Wai Chan[2]

Abstract

Cerebrospinal fluid (CSF) is an important biofluid for diagnosis of and research on neurological diseases. However, in-depth metabolomic profiling of CSF remains an analytical challenge due to the small volume of samples, particularly in small animal models. In this work, we report the application of a high-performance chemical isotope labeling (CIL) liquid chromatography–mass spectrometry (LC-MS) workflow for CSF metabolomics in *Gastrodia elata* and *Uncaria rhynchophylla* water extract (GUW)-treated experimental cerebral ischemia model of rat. The GUW is a commonly used Traditional Chinese Medicine (TCM) for hypertension and brain disease. This study investigated the amine- and phenol-containing biomarkers in the CSF metabolome. After GUW treatment for 7 days, the neurological deficit score was significantly improved with infarct volume reduction, while the integrity of brain histological structure was preserved. Over 1957 metabolites were quantified in CSF by dansylation LC-MS. The analysis of this comprehensive list of metabolites suggests that metabolites associated with oxidative stress, inflammatory response, and excitotoxicity change during GUW-induced alleviation of ischemic injury. This work is significant in that (1) it shows CIL LC-MS can be used for in-depth profiling of the CSF metabolome in experimental ischemic stroke and (2) identifies several potential molecular targets (that might mediate the central nervous system) and associate with pharmacodynamic effects of some frequently used TCMs.

Keywords: middle cerebral artery occlusion, cerebrospinal fluid, natural product extract, metabolomics, chemical isotope labeling, LC-MS

Introduction

Stroke is the second leading cause of death worldwide and the most frequent cause of long-term disability. In 2013, 15 million people suffered from stroke and 5.8 million of them died from cerebral stroke (Go, 2013). Therefore, it is an urgent need to develop preventive or treatment regimens for stroke. Among the natural product extract regimens, water extract of *Gastrodia elata* and *Uncaria rhynchophylla* (GUW) has the potential for treatment of cerebral ischemia, which is the major type of stroke. GUW extract is simplified and modified from *Gastrodia-Uncaria* decoction, a commonly used Traditional Chinese Medicine (TCM) prescription for hypertension treatment (Zhang et al., 2012). Several studies have reported that *Gastrodia elata* (GE) extracts provided protective effect against ischemia (Duan et al., 2015; Tsai et al., 2011) and beta-amyloid (Aβ)-induced neuronal apoptosis (Ng et al., 2013). Meanwhile, extracts of *Uncaria rhynchophylla* (UR) demonstrated neuroprotective effects against cerebral ischemia in rat (Jang et al., 2014; Jo et al., 2008).

Multiomic integrative biology is an emerging research scope to study stroke and TCM treatment (Black et al., 2015; Yun et al., 2012). To study the effects of drug or natural product extract treatment of ischemia stroke in animal models, metabolomic profiling of biofluids was used to correlate the metabolic changes with the efficiency of a treatment. For example, a study analyzed the serum metabolites of galangin, active ingredient of many TCM herbs, to elucidate its treatment effect on an experimental cerebral ischemia rat model (Gao et al., 2013). Similar analytical method was also deployed to study the use of a TCM prescription, Yiqijiedu Formulae, against middle cerebral artery occlusion (MCAO)-induced stroke in rats (Gao et al., 2014). The other examples include metabolomic study of brain tissue samples after treatment with Buyang Huanwu Tang Decoction on middle cerebral

[1]Department of Chemistry, University of Alberta, Edmonton, Alberta, Canada.
[2]School of Chinese Medicine, The Chinese University of Hong Kong, Shatin, New Territories, Hong Kong.
*Cofirst authors with equal contribution.

ischemic/reperfusion-induced stroke in mice (Chen et al., 2012) and the metabolomic study of serum and brain tissue extracts by ^{1}H NMR to investigate the neuroprotective effects of Huang-Lian-Jie-Du-Decoction on an MCAO stroke rat model (Wang et al., 2014).

In the metabolomic study of TCMs, blood is the commonly used sample for various types of diseases (Li et al., 2013b), whereas brain homogenate is mainly for investigation related to neurological disease (Wei et al., 2015). Cerebrospinal fluid (CSF) can act as an important medium for discovering potential biomarkers and their metabolites related to stroke or its treatment. Owing to a limited availability of CSF from a rat, a sensitive platform is essential for metabolomic profiling. On the other hand, accurate and precise quantification of individual metabolite concentration is critical to monitor small metabolic changes caused by the effective treatment of ischemia stroke. To fulfill these requirements, we have developed a high-performance chemical isotope labeling (CIL) liquid chromatography–mass spectrometry (LC-MS) method for quantitative metabolomics using rat CSF. In this report, we describe the CIL LC-MS workflow. The application of dansylation LC-MS for studying the amine/phenol submetabolome (i.e., a set of metabolites that contains a same functional group in a given biological system) and differential metabolites associated with GUW treatment was performed by analyzing CSF samples collected from the MCAO rat model. These metabolomic data supported the protective mechanism of GUW against cerebral ischemia. The study established a platform to detect the general rat CSF-related metabolites for studying neurological metabolomics.

Materials and Methods

Workflow for rat CSF metabolomics

The overall workflow for rat CSF metabolomics based on high-performance CIL LC-MS is shown in Figure 1. Briefly, individual samples were labeled by ^{12}C-dansylation, while a pooled CSF sample was prepared by mixing aliquots of individual samples, followed by labeling of ^{13}C-dansylation. The ^{13}C-labeled pool was spiked to all the ^{12}C-labeled individual samples in equal molar amounts as a global standard. The resultant mixtures were separately analyzed using LC-MS to produce mass spectra, where all the ^{13}C-/^{12}C-labeled metabolite peaks were shown in pairs. The intensity ratio between the ^{12}C-peak from a sample and the ^{13}C-peak from the pool within a pair reflected the relative concentration difference of the metabolite present in the individual sample versus the pooled sample. The ratio values found in specific group of sample for the peak pair of a specific metabolite reflected the concentration differences of this metabolite in these samples. After extracting all the peak pairs and their corresponding peak ratios, a metabolite-intensity table was constructed. The data in this table were exported for statistical analysis, including group separation based on the quantitative metabolome profile differences and determination of significant metabolites.

Herbal extracts

Raw herbal medicines, GE and UR, were purchased from Zhixin Medicine Health Co. (Guangdong, China). GUW was a mixture of GE and UR at a ratio of 3:4 (w/w). To prepare GUW extract, 107.1 g of GE was immersed in 2.5 L distilled

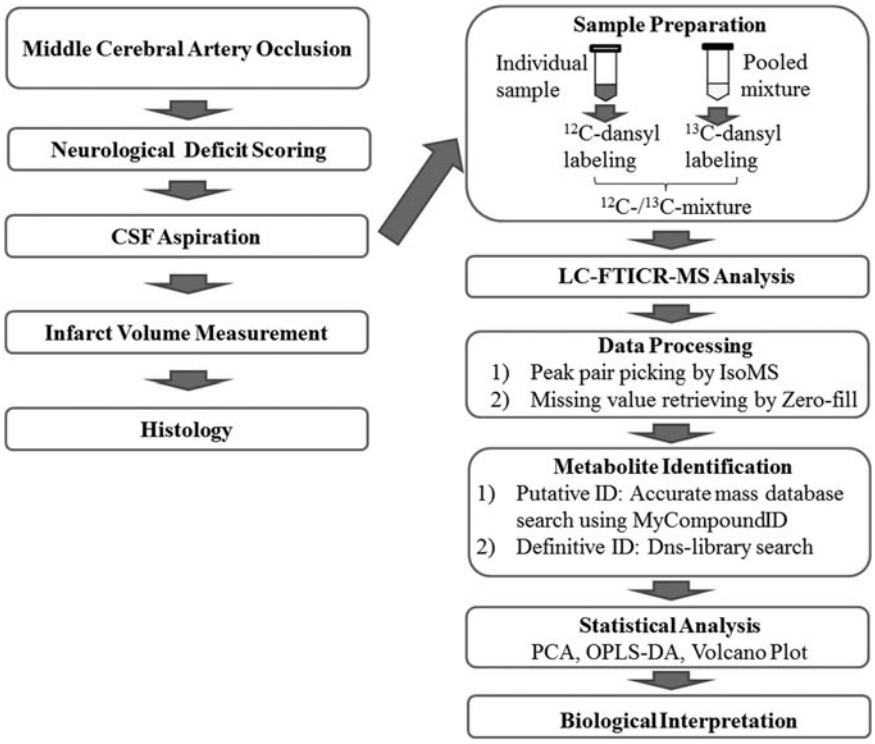

FIG. 1. Workflow for the whole study. CSF, cerebrospinal fluid; LC-FTICR-MS, liquid chromatography/Fourier transform ion cyclotron resonance mass spectrometry; OPLS-DA, orthogonal partial least squares discriminant analysis; PCA, principal component analysis.

water for 60 min and then boiled for 45 min; 142.9 g of UR was added to the mixture and was further boiled for another 15 min. The extract was concentrated under reduced pressure to yield dry powder of 33.25 g.

Animal model

Male Sprague-Dawley rats (260–280 g) were used in the study. The animals were housed in a 12-h light–12-h dark cycle with food and water available *ad libitum.* All experimental animal procedures were performed according to the approval from the animal experimentation ethics committee of The Chinese University of Hong Kong (AEEC ref number: 11/068/MIS-5).

Rats were randomly divided into three groups: the GUW treatment group, control, and sham group. Each group consisted of 10 animals. The rats were anesthetized with 400 mg/kg chloral hydrate through intraperitoneal injection. The cerebral blood flow (CBF) was monitored by laser Doppler flowmetry (PeriFlux System 5000; Perimed AB, Stockholm, Sweden) intraoperatively. After that, MCAO was done. Briefly, the external cerebral artery (ECA) and its branches were exposed and ligated. Then, a 4-0 nylon suture with a round tip was directed distally up toward the internal cerebral artery (ICA) to a distance of 17.5 ± 0.5 mm from the common carotid artery (CCA) to occlude the middle cerebral artery. A 60% reduction of CBF from the baseline was indicated as a successful MCAO. After 120 min, the nylon filament was gently removed to allow reperfusion. For the sham-operated rats, the left CCA and ECA were exposed without inserting the filament into the ICA. After surgery, the rats from the GUW treatment group were treated with 288.6 mg/kg of GUW by oral gavage once daily for seven consecutive days. Rats from control and sham groups were orally administered with distilled water as vehicle.

Neurological and histopathological measurement

The neurological deficit score was measured by modified Bederson's scoring system to assess the prognosis of GUW treatment of cerebral ischemia on days 1, 2, 4, 6, and 7 poststroke (Xian et al., 2016). The scoring was assessed as follows: Score 1: contralateral limb flexion; Score 2: decreased resistance to lateral push to the left; Score 3: contralateral circling to the left only; and Score 4: spontaneous circling.

For histopathological assessment, on day 7, 1 h after administering the final treatment of GUW or vehicle, the brain was perfused transcardially with phosphate-buffered saline (PBS) for 30 min, followed by 4% paraformaldehyde for 10 min. The brain was harvested and embedded in paraffin wax. Hematoxylin and eosin and cresyl violet staining were done on brain coronal sections of 6 μm thickness separately.

Brain infarct volume was quantified by 2% 2, 3, 5-triphenyltetrazolium chloride (TTC) staining (Xian et al., 2016). Coronal sections of 2 mm thickness were stained with 2% TTC solution in PBS and incubated at 37°C for 20 min. Infarct volume was calculated according to the following formula:

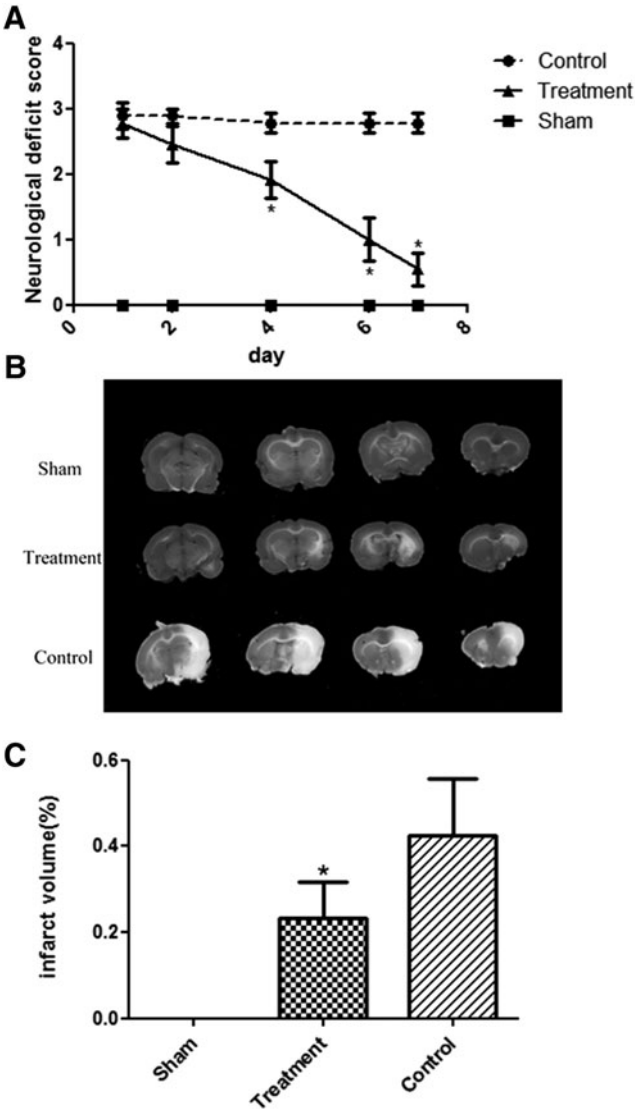

FIG. 2. **(A)** Neurological deficit score measurement results from different groups. **(B)** Triphenyltetrazolium chloride-stained brain slices (four sections within a brain tissue). **(C)** The percentage of brain infarction for different groups of rats on day 7 after MCAO. Data are mean ± standard deviation ($n = 10$). *$p < 0.001$ from comparison of treatment versus control. MCAO, middle cerebral artery occlusion.

CSF collection, dansyl labeling, and sample normalization

On day 7 poststroke, CSF was aspirated without blood contamination after general anesthesia and stored in −80°C freezer before analysis. The volume of CSF collected ranged from 30 to 100 μL per rat. Supplementary Data describe the dansylation protocol developed to handle a small volume of CSF samples. Briefly, the lyophilized CSF samples were redissolved in 75 μL of water. The samples were then vortexed

$$\textbf{Infarct Volume} = \frac{\textbf{Left hemisphere} - (\textbf{Right hemisphere} - \textbf{Measured infarct})}{\textbf{Left hemisphere}}$$

for 10 sec and followed by centrifugation at 20,800 × *g* for 10 min. Each CSF sample was aliquoted out into three vials at equal volumes. Two vials were used for the experimental duplicates, and one vial was used for preparing the pooled sample. To normalize the amount of individual samples used for comparative metabolomics, the total concentration of dansyl-labeled metabolites in each individual or pooled sample was determined using a liquid chromatography-ultraviolet (LC-UV) method (Wu and Li, 2012).

LC-MS analysis

Supplementary Data provide more detailed information on LC-MS analysis. In brief, after mixing an equal amount of ^{12}C-labeled sample and ^{13}C-labeled pool, the mixture was analyzed using an Agilent 1100 series HPLC system (Palo Alto, CA, USA) coupled with a Bruker 9.4-Tesla Apex-Qe Fourier transform ion cyclotron resonance (FTICR) mass spectrometer (Billerica, MA, USA). LC mobile phase A was 0.1% (v/v) LC-MS grade formic acid in 5% (v/v) LC-MS grade acetonitrile (ACN), and mobile phase B was 0.1% (v/v) LC-MS grade formic acid in LC-MS grade ACN. The flow rate was 180 μL/min and running time was 28 min. The gradient elution profile was as follows: t = 0 min, 20% B; t = 3.50 min, 35% B; t = 18.00 min, 65% B; t = 21.00 min, 95% B; t = 21.50 min, 95% B; t = 23.00 min, 98% B; t = 24.00 min, 98% B; t = 26.50 min, 99% B; and t = 28.00 min, 99% B. The sample injection volume was 6 μL and the flow was split 1:2. A 60 μL/min flow was loaded to the electrospray ionization source of the MS, while the rest of the flow was discarded (Guo and Li, 2009).

Data processing and metabolite identification

The MS peaks with S/N ≥3 in the raw LC-MS data were exported using Bruker Data Analysis software. After that, IsoMS (Zhou et al., 2014) was used to pick the peak pair with S/N ≥10 from real metabolites; to filter out redundant pairs (from salt adducts, dimers, multimers, etc.); and to retain only protonated molecular ion pair from one metabolite. The ^{13}C-/^{12}C-peak intensity ratio was calculated for each peak pair for the relative intensity information. The intensity ratio of same peak pairs across different samples was aligned together to produce a metabolite-intensity table using IsoMS-align (Zhou et al., 2014). Missing values in the table were then refilled from the raw LC-MS data with the Zero-fill program (Huan and Li, 2015). Definitive metabolite identification was performed by matching retention time (RT) and m/z with the dansyl standards library in the DnsID program (Huan et al., 2015) with an m/z tolerance of 5 ppm and RT tolerance of 15 sec. Putative metabolite identification was performed by matching accurate mass of a peak pair against the human metabolome libraries (with zero or one reaction) using MyCompoundID (MCID) with a mass tolerance of 5 ppm.

Statistical analysis

Before multivariate analysis, missing values in the metabolite-intensity tables were replaced by peak ratio means to eliminate any potential statistical bias and all the data were preprocessed using autoscaling (i.e., each value subtracted the mean and then was divided by the peak ratio standard deviation [SD]). Multivariate analysis was performed on SIMCA-P+ 12.0 software (Umetrics, Umea, Sweden). Statistical significance was measured using unpaired nonparametric *t*-test. Volcano plot was constructed using Excel and ProginPro 8.5 (OriginLab). For the biological data, all results are given as mean ± SD. Data for multiple comparisons were analyzed by one-way analysis of variance, followed by Dunnett's multiple comparison tests (GraphPad Prism 5.0 software; San Diego, CA, USA).

Results

Effects of GUW treatment after MCAO

The neurological deficit score of the control group remained almost stable at Score 3 for 7 days post-MCAO (Fig. 2A). Starting from day 4, the score of the GUW

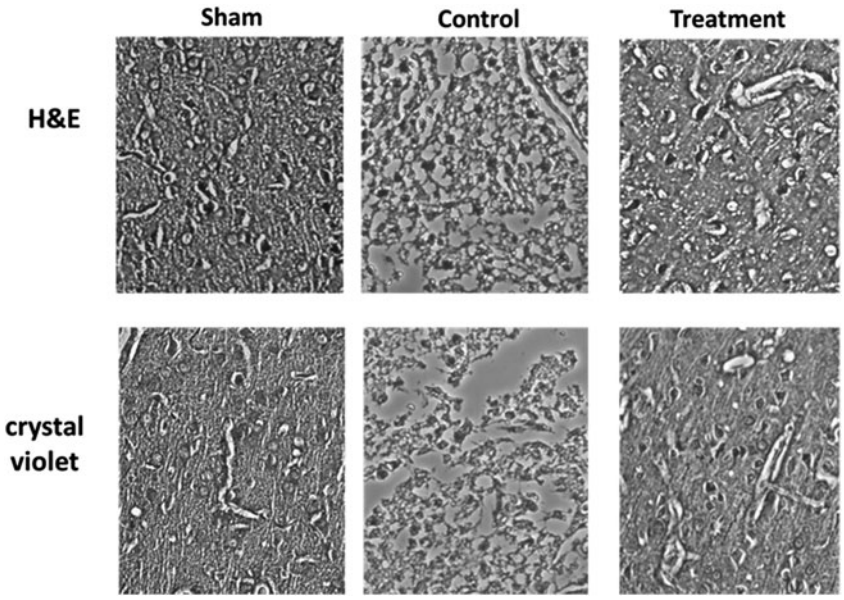

FIG. 3. Images of H&E and cresyl *violet*-stained coronal brain sections of rats on day 7 after MCAO. H&E, hematoxylin and eosin.

treatment group was significantly reduced compared with the control group. The brain section images on day 7 showed that MCAO caused infarct in cerebral cortex, hippocampus, and basal ganglia (Fig. 2B). The brain infarct volume was 40.6% in the control group. With GUW treatment, the infarct volume was reduced by 54.8% of the control group on day 7 ($p < 0.001$, Fig. 2C). The structure integrity of GUW-treated brain was maintained and did not have significant difference compared with the sham group, while loss of integrity and neuron numbers were observed at the brain cortex after MCAO-induced injury on rat (Fig. 3).

Sample amount normalization

To compare concentrations of individual metabolites present in CSF samples collected from different rats, it is important to make sure that the total amount of metabolites in different samples is normalized. We used a dansylation LC-UV normalization method to normalize the samples. The average concentrations of labeled metabolites in sham, control, and treatment groups were determined to be 0.22 ± 0.08, 0.26 ± 0.04, and 0.25 ± 0.04 mM, respectively (Fig. 4A). On average, there are no significant concentration differences in concentration of labeled metabolites among the three groups. However, the concentration difference among the redissolved samples can be quite large. For example, in the sham group, the difference between the highest and lowest concentrated samples was 4.5-fold. This large difference indicates the importance of performing sample amount normalization before quantitative metabolomic analysis.

LC-MS profiling of the CSF metabolome

Figure 4B shows a representative ion chromatogram obtained by injecting an optimal amount (2.5 nmol) of a ^{13}C-/^{12}C-labeled CSF mixture. Metabolites were detected across the entire separation time window using the optimized chromatographic conditions. Many chromatographic peaks with high S/N ratios were shown, demonstrating that dansylation afforded sensitive detection of metabolites from a dilute CSF sample. Figure 4C shows a typical mass spectrum displaying a pair of protonated molecules from a differentially labeled metabolite, dansyl (Dns)-phenylalanine. The peak intensity ratio (m/z 399.1373 vs. m/z 401.1437) reflected the relative concentration of the metabolite in the ^{12}C-labeled sample versus the ^{13}C-pool. In this work, experimental duplicate was carried out for each CSF sample. Totally, 48 LC-MS runs were performed for the 24 CSF samples. In total, 1957 peak pairs or metabolites were found in these runs with an average of 1360 ± 133 ($n = 48$) pairs per run. Figure 4D shows the number of pairs detected as a function of percentage of common pairs found in these runs. There were 1545 pairs (79% of the total number) in more than 50% of the runs, demonstrating that many metabolites could be consistently quantified using dansylation LC-MS. These pairs were used for statistical analysis. There were 745 pairs commonly detected in all the runs.

By searching the 1957 peak pairs against the dansyl library consisting of 273 labeled standards with the use of mass tolerance of 5 ppm and RT tolerance of 15 sec, 81 metabolites were positively identified based on mass and RT matches (Supplementary Table S1). Using MCID, an MS search based on accurate mass of peak pairs with mass tolerance of 5 ppm, 586 metabolites were putatively identified using the HMDB library (Supplementary Table S2) and additionally 659 metabolites were putatively identified using the predicted human metabolite library with one reaction (Supplementary Table S3). Thus, of the 1957 pairs, a total of 1326 metabolites (68%) could be positively or putatively identified.

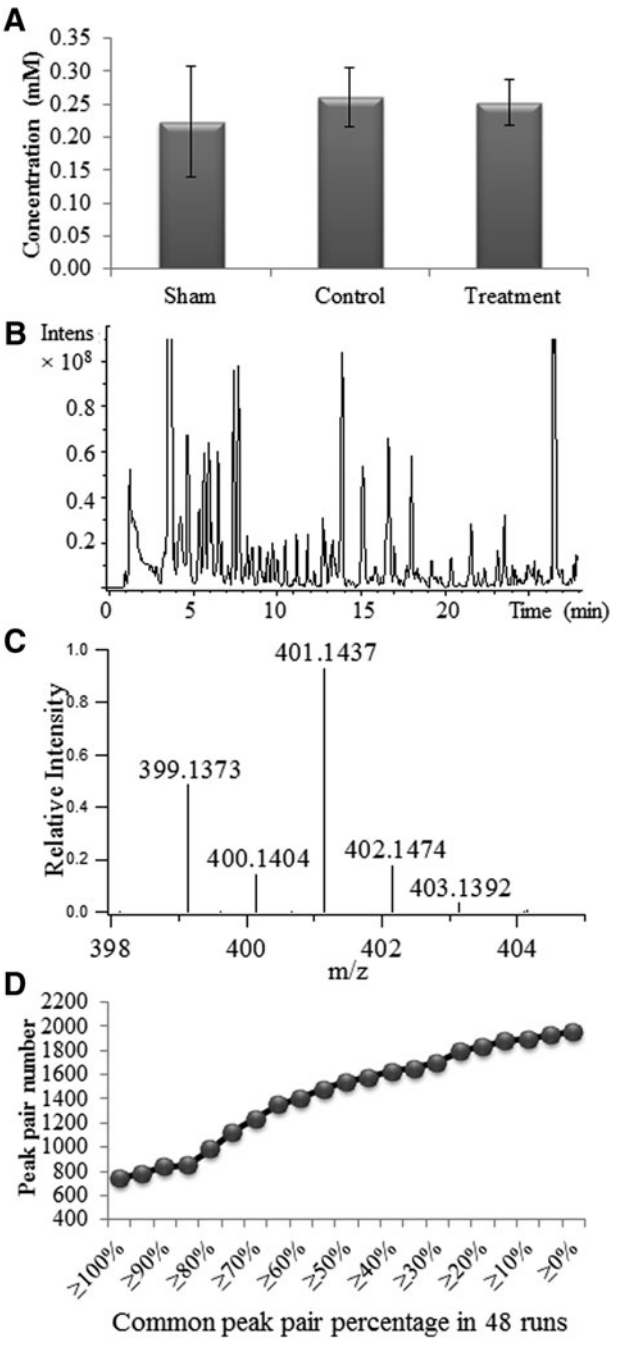

FIG. 4. **(A)** LC-UV quantification of the labeled metabolites in CSF samples. **(B)** Base peak ion chromatogram from LC-FTICR-MS analysis of a ^{13}C-/^{12}C-dansyl-labeled CSF sample. **(C)** Mass spectrum showing a pair of ^{13}C-/^{12}C-dansyl-labeled metabolites. **(D)** Number of peak pairs as a function of common peak pair percentage across all the 48 LC-MS runs.

Statistical analysis of CSF metabolomes

For the metabolomic data set generated using dansylation LC-MS, principal component analysis was used to provide an overview of the sham, control, and treatment groups (Fig. 5A). Some separations of the groups were identified. Figure 5B displays the orthogonal partial least squares discriminant analysis (OPLS-DA) score plot of the three groups showing a clear group separation ($R^2Y = 0.923$, $Q^2 = 0.707$). The OPLS-DA score plot of control versus sham group in Figure 5C shows a separation ($R^2Y = 0.982$, $Q^2 = 0.938$). The control and treatment groups are also clearly separated ($R^2Y = 0.991$, $Q^2 = 0.784$) (Fig. 5D). The volcano plots of these binary comparisons are shown in Figure 5E and F.

To increase the confidence of determining the metabolites that contributed to group separation, we combined the significant metabolites found using OPLS-DA (VIP score ≥1.5) and volcano plot (fold-change ≥1.5 or ≤0.67 and $p \leq 0.01$). There were 545 significant metabolites separating the control and sham groups (Supplementary Table S4), while 96 metabolites were deemed to be significant in separating the control and GUW treatment groups (Supplementary Table S5). There are considerably more significant changes of metabolites in control versus sham than control versus treatment groups, suggesting that a large fraction of the metabolite concentration changes happened after stroke insult. Even though the GUW treatment could help reduce the stroke effect, some of the metabolic changes were irreversible.

Discussion

CSF is an important body fluid for discovering potential biomarkers in central nervous system diseases. In this study, we developed and applied a quantitative metabolomic profiling workflow based on CIL LC-MS to study the metabolomic changes in treatment of experimental stroke using natural product extracts. Unlike conventional LC-MS, CIL LC-MS uses chemical labeling to introduce differential isotopic mass tags to metabolites in comparative samples. There are a number of labeling reagents developed for targeting different classes of metabolites (Bueschl et al., 2013; Dai et al., 2012; Hao et al., 2015; Yu et al., 2015). A rational design of the labeling groups leads to concomitant improvements in separation, detection, quantification, and identification (Guo and Li, 2009, 2010). Such high-performance labeling methods, including dansylation LC-MS targeting the amine/phenol submetabolome (Guo and Li, 2009) where detection sensitivity improvement of over 10- to 1000-fold can be achieved, allow a high coverage detection of the submetabolome. Using dansylation LC-MS, over 1957 metabolites could be detected and about 80% of them could be consistently quantified over 50% of the 48 LC-MS runs of 24 rat CSF samples. Therefore, the workflow reported herein (Fig. 1) should be generally applicable to other types of metabolites. In our current workflow, regular LC-MS was used to analyze the labeled metabolites. Recently, it was demonstrated that CIL LC-MS can also be performed using nanoflow LC-MS, which offers the advantage of consuming an even smaller sample amount per test (Li et al., 2015). Thus, we

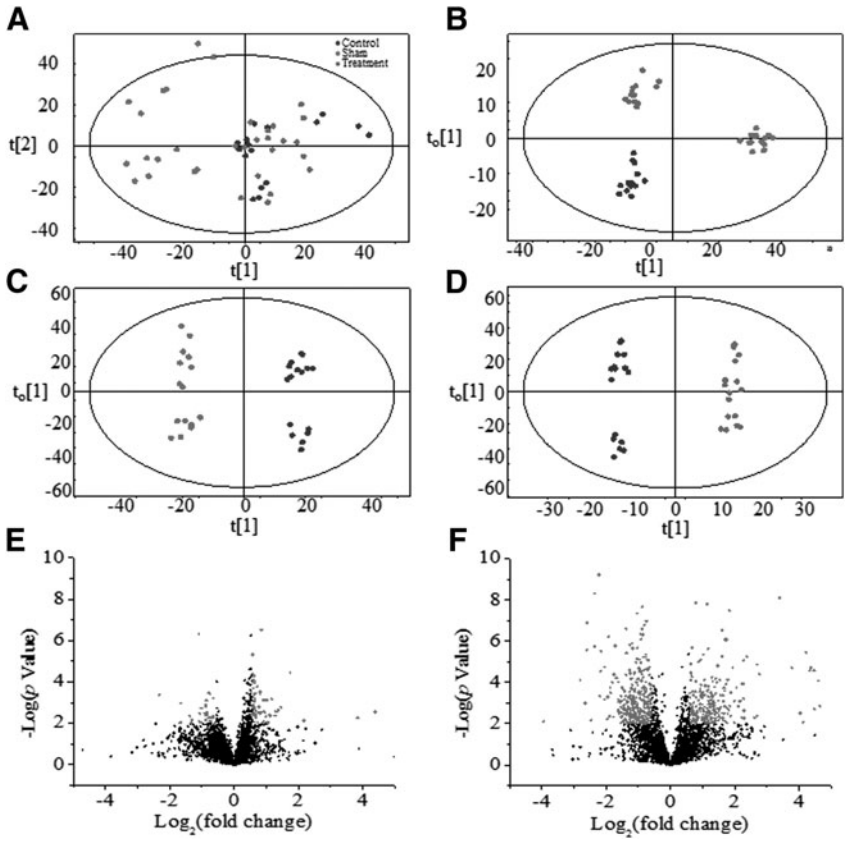

FIG. 5. **(A)** PCA score plot of three groups. OPLS-DA score plots of **(B)** three groups, **(C)** control versus sham, and **(D)** treatment versus control. Volcano plots of **(E)** control versus sham and **(F)** treatment versus control.

anticipate that with nanoflow LC-MS, the workflow shown in Figure 1 might adapt multiple labeling experiments of the same sample for quantitative rat CSF metabolomics with even greater coverage.

With the use of a natural product extract, GUW, this study has demonstrated the utility of dansylation LC-MS workflow for rat CSF stroke and its treatment-related metabolomics. Cerebral ischemia initiates a cascade of detrimental events, including glutamate-associated excitotoxicity; membrane lipid degradation; DNA damage; formation of reactive oxygen species (ROS); and acute inflammation, which lead to the disruption of cellular homeostasis and structural damage of ischemic brain tissue (Kim et al., 2014). Oxidative stress is one of the major causes leading to brain damage and following pathophysiological consequences (Chen et al., 2011; Uttara et al., 2009). Meanwhile, ROS, such as superoxide and hydroxyl radicals, produce systemic oxidative damage to lipids and proteins (Kalogeris et al., 2012) and direct consequence of excitotoxic stimulation during reperfusion of ischemic brain tissue (Demaurex and Scorrano, 2009).

GE and its active ingredients exhibit antioxidative effect against focal cerebral ischemia. Gastrodin is one of the major compounds to protect against cerebral ischemia by improving antioxidant and anti-inflammation activities (Peng et al., 2015). Additionally, 4-hydroxybenzaldehyde can activate antioxidative and GABAergic pathways (Jang et al., 2015). Furthermore, vanillin suppresses hydrogen peroxide-induced oxidative injury on PC12 cells (Kim et al., 2007). In our previous study, GUW treatment was found to upregulate the antioxidative pathway against oxygen–glucose deprivation (OGD)-induced injury on PC12 cells and MCAO rat (Xian et al., 2016). However, there was no study reporting about the changes in metabolite profiles of GUW and even GE during the neuroprotective events.

Most importantly, we definitively identified six metabolites having significant metabolic changes in either the control versus sham groups or the control versus treatment groups (Table 1). We found that MCAO led to the increase in levels of methylamine and xanthine (Fig. 6A, B). Methylamine is one of the endogenous aliphatic amines, which can be oxidized by semicarbazide-sensitive amine oxidase, leading to the production of toxic aldehydes such as formaldehyde, methylglyoxal, hydrogen peroxide, and ammonia (Xiao and Yu, 2009). It plays a significant role in central nervous system disturbances observed during renal and hepatic diseases and general toxicity caused by oxidative stress (Nunes et al., 2011, 2012). On the other hand, xanthine increases after stroke onset, and inhibition of xanthine product was beneficial to rescue brain tissue during cerebral ischemia through inhibiting ROS generation (Pacher et al., 2006). Interestingly, increased level of pyridoxamine in the MCAO control group was observed, which was decreased again in the GUW group (Fig. 6C). Pyridoxamine is an inhibitor of advanced glycation endproduct (AGE) (Miyashita et al., 2014), while AGE production was enhanced in ischemic injury (Takeshita et al., 2014). The possible explanation for this phenomenon might be that the high-level production of pyridoxamine might inhibit synthesis of AGE during early chronic phase of stroke, whereas the effective neuroprotection of GUW treatment in acute phase of stroke led to reduced level of pyridoxamine.

After the onset of cerebral ischemia, the inflammatory cascades are initiated within the infarct tissue, leading to secondary cell death in ischemic penumbra (Ouyang, 2013; Won et al., 2002). Microglia, macrophages, and leukocytes respond to the cascades and further carry out inflammatory events along with factors released by neurons and astrocytes (Boutin et al., 2001). Therefore, reducing oxidative stress and downregulating the inflammatory response are alternative therapeutic means for ischemic stroke. In our result, the amount of endogenous L-N-monomethylarginine (L-NMMA) (Fig. 6D) in the GUW treatment group was significantly greater than the MCAO control group. During the onset of ischemia, excessive increase in intracellular calcium leads to the generation of nitric oxide. Nitric oxide is converted to free radical form $ONOO^-$ by receiving ROS that further damages the brain (Bolanos and Almeida, 1999). Suppression of nitric oxide production is suggested to be one of the neuroprotective mechanisms. *In vivo* endogenous L-NMMA is a natural competitive inhibitor of inducible nitric oxide synthase (Tang et al., 2008). Previous studies reported that the active ingredients of UR, including rhynchophylline (Rhy), isorhynchophylline (Isorhy), and hirsutine, exhibit protective effect on stroke through inhibition of NO production (Jung et al., 2013; Yuan et al., 2009). Thus, the inhibitory effect of GUW on inflammation could be due to increase in the concentration of L-NMMA, which inhibits nitric oxide synthesis and the downstream apoptotic cascade.

In the ischemic stroke pathogenesis, excitotoxicity plays an important role. Glutamine synthetase (GS) is a key

Table 1. Significant Metabolites Identified in the Binary Comparisons Between the Control and Sham Groups and Between the Treatment and Control Groups

				Control/sham		*Treatment/control*	
No.	*Metabolite name*	*RT (min)*	*m/z light*	*Fold change*	p	*Fold change*	p
1	Methylamine	10.03	265.1002	2.07	7.4e-5	0.95	6.5e-2
2	Xanthine	9.37	386.0916	1.39	2.2e-2	0.78	7.1e-2
3	Pyridoxamine	20.00	318.1030	1.34	6.7e-2	0.49	2.6e-3
4	L-N-monomethylarginine	6.66	422.1860	0.50	6.8e-5	1.50	4.8e-6
5	Glutamine	4.06	380.1273	0.49	4.4e-8	1.45	5.0e-4
6	Histidine	18.64	389.1275	0.56	3.9e-4	1.32	1.3e-2

RT, retention time.

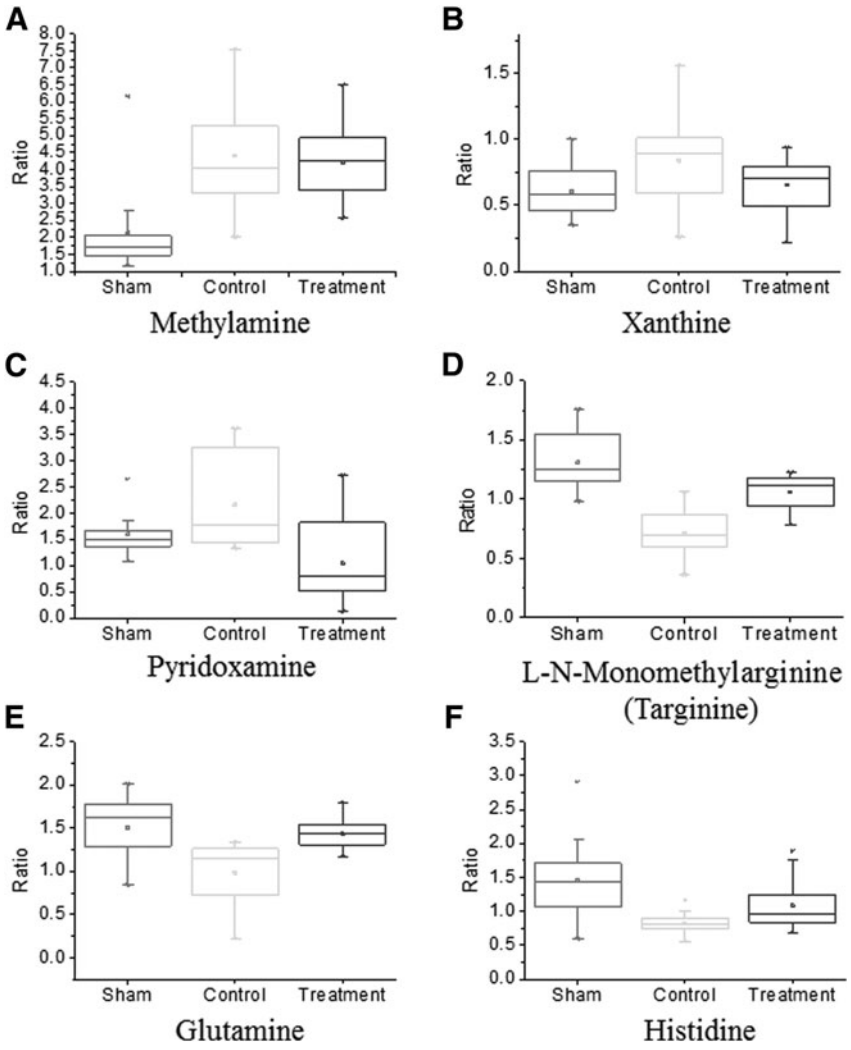

FIG. 6. Box plots of peak ratios (sample/pool) of six metabolites in the sham, control, and GUW treatment groups (see Table 1 for the data and comparison statistics). GUW, *Gastrodia elata* and *Uncaria rhynchophylla* water extract.

enzyme in the glutamate–glutamine pathway that regulates the extracellular concentration of glutamate in brain (Kosenko et al., 2003). GS expression was reduced after cerebral ischemia; in the meantime, the extracellular glutamate level was increased (Wang et al., 2013). The increased glutamate level mediates excitotoxicity in the ischemic brain (Davalos et al., 1997) due to continuous excitation by the neurotransmitter. From our results, the glutamine level was increased after treating MCAO rats with GUW (Fig. 6E), suggesting the increased conversion of glutamate to glutamine with the increase in GS activity. Histidine was reported to have neuroprotective effect after stroke onset through neuronal nitric oxide synthase inhibition (Tang et al., 2007). Histidine can undergo decarboxylation to form histamine, which mediates allergic and inflammatory responses (Tang et al., 2007). Upregulating histidine concentration increases anti-inflammatory effect after stroke onset (Simon et al., 2013). Furthermore, histamine upregulated GS expression in primary cultured cortical astrocytes after exposure of OGD insult (Wang et al., 2013). Thus, histidine-derived histamine could reduce the level of glutamate and alleviate the excitotoxicity induced by glutamate. Our results indicated that the level of histidine (Fig. 6F) and glutamine was reduced after MCAO injury. With the treatment with GUW, the level of histidine and glutamine was increased. The result indicated that GUW treatment possessed anti-inflammatory and antiexcitotoxic effects against cerebral ischemia.

In the reported metabolomic studies of natural product extract treatment of cerebral ischemia, they mostly focused on the metabolites in brain tissue or serum (Chen et al., 2012; Gao et al., 2014; Wang et al., 2014). Various TCM formulae were applied prestroke (Gao et al., 2014), acute phase (Chen et al., 2012), and early chronic phase of stroke (Wang et al., 2014) in different studies. Our study is the first investigation of the metabolic profile and the networks in CSF collected during the early chronic phase of stroke after treatment with TCM formulae. Only xanthine and glutamine found in our study were also detected in another study (Wang et al., 2014), even though the applied formulae were totally different from this study. They might be candidates of biomarkers in recovery of stroke, especially the amount of glutamine from aspirated CSF and serum could be measured (Wang et al., 2014). On the other hand, the other four metabolites, methylamine, pyridoxamine, histidine, and L-NMMA, require further analysis to characterize their uniqueness in GUW

treatment of cerebral ischemia. Overall, all six metabolites could be the target of interest to investigate GUW treatment in future clinical studies.

Our report shows that the treatment with GUW protected the brain tissue against cerebral ischemia, possibly through antioxidative pathways through inhibition of xanthine and methylamine, and induction of pyridoxamine production against ROS generation. Among the changes, the pyridoxamine–histidine–glutamine-related pathway could contribute to antiexcitotoxic and anti-inflammatory effects of GUW. Further studies are warranted to elucidate the regulation of therapeutic mechanism of GUW in cerebral ischemia.

In all, this work is significant in that (1) it shows CIL LC-MS can be used for in-depth profiling of the CSF metabolome in experimental ischemic stroke and (2) identifies several potential molecular targets that might mediate the central nervous system associated with pharmacodynamic effects of some frequently used TCMs.

Acknowledgments

This study was supported by the Health and Medical Research Fund, HKSAR (Ref. No. 11120381), and the Natural Sciences and Engineering Research Council of Canada, the Canadian Institutes for Health Research, the Canada Research Chairs program, Genome Canada, Genome Alberta, and Alberta Innovates.

Author Disclosure Statement

The authors declare that no conflicting financial interests exist.

References

Black M, Wang W, and Wang W. (2015). Ischemic stroke: From next generation sequencing and GWAS to community genomics? OMICS 19, 451–460.

Bolanos JP, and Almeida A. (1999). Roles of nitric oxide in brain hypoxia-ischemia. Biochim Biophys Acta 1411, 415–436.

Boutin H, LeFeuvre RA, Horai R, et al. (2001). Role of IL-1alpha and IL-1beta in ischemic brain damage. J Neurosci 21, 5528–5534.

Bueschl C, Krska R, Kluger B, and Schuhmacher R. (2013). Isotopic labeling-assisted metabolomics using LC-MS. Anal Bioanal Chem 405, 27–33.

Chen HJ, Shen YC, Lin CY, et al. (2012). Metabolomics study of Buyang Huanwu Tang decoction in ischemic stroke mice by H-1 NMR. Metabolomics 8, 974–984.

Chen H, Yoshioka H, Kim GS, et al. (2011). Oxidative stress in ischemic brain damage: Mechanisms of cell death and potential molecular targets for neuroprotection. Antioxid Redox Signal 14, 1505–1517.

Dai WD, Huang Q, Yin PY, et al. (2012). Comprehensive and highly sensitive urinary steroid hormone profiling method based on stable isotope-labeling liquid chromatography mass spectrometry. Anal Chem 84, 10245–10251.

Davalos A, Castillo J, Serena J, and Noya M. (1997). Duration of glutamate release after acute ischemic stroke. Stroke 28, 708–710.

Demaurex N, and Scorrano L. (2009). Reactive oxygen species are NOXious for neurons. Nat Neurosci 12, 819–820.

Duan X, Wang W, Liu X, et al. (2015). Neuroprotective effect of ethyl acetate extract from *Gastrodia elata* against transient focal cerebral ischemia in rats induced by middle cerebral artery occlusion. J Tradit Chin Med 35, 671–678.

Gao J, Chen C, Chen JX, et al. (2014). Synergism and rules of the new combination drug Yiqijiedu Formulae (YQJD) on ischemic stroke based on amino acids (AAs) metabolism. Sci Rep 4, 5149.

Gao J, Yang H, Chen J, et al. (2013). Analysis of serum metabolites for the discovery of amino acid biomarkers and the effect of galangin on cerebral ischemia. Mol Biosyst 9, 2311–2321.

Go AS. (2013). Heart disease and stroke statistics-2013 update: A report from the American heart association. Circulation 127, E841–E841.

Guo K, and Li L. (2009). Differential 12C-/13C-Isotope dansylation labeling and fast liquid chromatography/mass spectrometry for absolute and relative quantification of the metabolome. Anal Chem 81, 3919–3932.

Guo K, and Li L. (2010). High-performance isotope labeling for profiling carboxylic acid-containing metabolites in biofluids by mass spectrometry. Anal Chem 82, 8789–8793.

Hao L, Zhong XF, Greer T, Ye H, and Li LJ. (2015). Relative quantification of amine-containing metabolites using isobaric N,N-dimethyl leucine (DiLeu) reagents via LC-ESI-MS/MS and CE-ESI-MS/MS. Analyst 140, 467–475.

Huan T, and Li L. (2015). Counting missing values in a metabolite-intensity data set for measuring the analytical performance of a metabolomics platform. Anal Chem 87, 1306–1313.

Huan T, Wu YM, Tang CQ, Lin GH, and Li L. (2015). DnsID in MyCompoundID for rapid identification of dansylated amine- and phenol-containing metabolites in LC-MS-based metabolomics. Anal Chem 87, 9838–9845.

Jang JH, Son Y, Kang SS, et al. (2015). Neuropharmacological potential of *Gastrodia elata* blume and its components. Evid Based Complement Alternat Med 2015, 309261.

Jang JY, Choi YW, Kim HN, et al. (2014). Neuroprotective effects of a novel single compound 1-methoxyoctadecan-1-ol isolated from Uncaria sinensis in primary cortical neurons and a photothrombotic ischemia model. PLoS One 9, e85322.

Jo KJ, Cha MR, Lee MR, Yoon MY, and Park HR. (2008). Methanolic extracts of *Uncaria rhynchophylla* induce cytotoxicity and apoptosis in HT-29 human colon carcinoma cells. Plant Foods Hum Nutr 63, 77–82.

Jung HY, Nam KN, Woo BC, et al. (2013). Hirsutine, an indole alkaloid of *Uncaria rhynchophylla*, inhibits inflammation-mediated neurotoxicity and microglial activation. Mol Med Rep 7, 154–158.

Kalogeris T, Baines CP, Krenz M, and Korthuis RJ. (2012). Cell biology of ischemia/reperfusion injury. Int Rev Cell Mol Biol 298, 229–317.

Kim HJ, Hwang IK, and Won MH. (2007). Vanillin, 4-hydroxybenzyl aldehyde and 4-hydroxybenzyl alcohol prevent hippocampal CA1 cell death following global ischemia. Brain Res 1181, 130–141.

Kim JY, Kawabori M, and Yenari MA. (2014). Innate inflammatory responses in stroke: Mechanisms and potential therapeutic targets. Curr Med Chem 21, 2076–2097.

Kosenko E, Llansola M, Montoliu C, et al. (2003). Glutamine synthetase activity and glutamine content in brain: Modulation by NMDA receptors and nitric oxide. Neurochem Int 43, 493–499.

Li L, Li RH, Zhou JJ, et al. (2013a). MyCompoundID: Using an evidence-based metabolome library for metabolite identification. Anal Chem 85, 3401–3408.

Li Y, Liu H, Wu X, et al. (2013b). An NMR metabolomics investigation of perturbations after treatment with Chinese herbal medicine formula in an experimental model of sepsis. OMICS 17, 252–258.

Li ZD, Tatlay J, and Li L. (2015). Nanoflow LC-MS for high-performance chemical isotope labeling quantitative metabolomics. Anal Chem 87, 11468–11474.

Miyashita M, Arai M, Kobori A, et al. (2014). Clinical features of schizophrenia with enhanced carbonyl stress. Schizophr Bull 40, 1040–1046.

Ng CF, Ko CH, Koon CM, et al. (2013). The aqueous extract of rhizome of *Gastrodia elata* protected drosophila and PC12 cells against beta-amyloid-induced neurotoxicity. Evid Based Complement Alternat Med 2013, 516741.

Nunes SF, Figueiredo IV, Pereira JS, et al. (2011). Monoamine oxidase and semicarbazide-sensitive amine oxidase kinetic analysis in mesenteric arteries of patients with type 2 diabetes. Physiol Res 60, 309–315.

Nunes SF, Figueiredo IV, Pereira JS, Lopes MC, and Caramona MM. (2012). Correlation between total nitrite/nitrate concentrations and monoamine oxidase (types A and B) and semicarbazide-sensitive amine oxidase enzymatic activities in human mesenteric arteries from non-diabetic and type 2 diabetic patients. Braz J Med Biol Res 45, 20–24.

Ouyang YB. (2013). Inflammation and stroke. Neurosci Lett 548, 1–3.

Pacher P, Nivorozhkin A, and Szabo C. (2006). Therapeutic effects of xanthine oxidase inhibitors: Renaissance half a century after the discovery of allopurinol. Pharmacol Rev 58, 87–114.

Peng ZW, Wang SQ, Chen GJ, et al. (2015). Gastrodin alleviates cerebral ischemic damage in mice by improving anti-oxidant and anti-inflammation activities and inhibiting apoptosis pathway. Neurochem Res 40, 661–673.

Shen W, Han W, Li Y, et al. (2016). Development of chemical isotope labeling liquid chromatography mass spectrometry for silkworm hemolymph metabolomics. Anal Chim Acta [Epub ahead of print]; DOI: 10.1016/j.aca.2016.06.004.

Simon A, Karbach S, Habermeier A, and Closs EI. (2013). Decoding the substrate supply to human neuronal nitric oxide synthase. PLoS One 8, e67707.

Takeshita T, Nakagawa S, Tatsumi R, et al. (2014). Cilostazol attenuates ischemia-reperfusion-induced blood-brain barrier dysfunction enhanced by advanced glycation endproducts via transforming growth factor-beta 1 signaling. Mol Cell Neurosci 60, 1–9.

Tang SC, Arumugam TV, Cutler RG, et al. (2007). Neuroprotective actions of a histidine analogue in models of ischemic stroke. J Neurochem 101, 729–736.

Tang WH, Tong W, Shrestha K, et al. (2008). Differential effects of arginine methylation on diastolic dysfunction and disease progression in patients with chronic systolic heart failure. Eur Heart J 29, 2506–2513.

Tsai CF, Huang CL, Lin YL, et al. (2011). The neuroprotective effects of an extract of *Gastrodia elata*. J Ethnopharmacol 138, 119–125.

Uttara B, Singh AV, Zamboni P, and Mahajan RT. (2009). Oxidative stress and neurodegenerative diseases: A review of upstream and downstream antioxidant therapeutic options. Curr Neuropharmacol 7, 65–74.

Wang PR, Wang JS, Yang MH, and Kong LY. (2014). Neuroprotective effects of Huang-Lian-Jie-Du-Decoction on ischemic stroke rats revealed by H-1 NMR metabolomics approach. J Pharmaceut Biomed 88, 106–116.

Wang XF, Hu WW, Yan HJ, et al. (2013). Modulation of astrocytic glutamine synthetase expression and cell viability by histamine in cultured cortical astrocytes exposed to OGD insults. Neurosci Lett 549, 69–73.

Wei L, Xue R, Zhang P, et al. (2015). (1)H NMR-based metabolomics and neurotoxicity study of cerebrum and cerebellum in rats treated with cinnabar, a Traditional Chinese Medicine. OMICS 19, 490–498.

Won SJ, Kim DY, and Gwag BJ. (2002). Cellular and molecular pathways of ischemic neuronal death. J Biochem Mol Biol 35, 67–86.

Wu YM, and Li L. (2012). Determination of total concentration of chemically labeled metabolites as a means of metabolome sample normalization and sample loading optimization in mass spectrometry-based metabolomics. Anal Chem 84, 10723–10731.

Xian JW, Choi AY, Lau CB, et al. (2016). *Gastrodia* and *Uncaria* (tianma gouteng) water extract exerts antioxidative and antiapoptotic effects against cerebral ischemia *in vitro* and *in vivo*. Chin Med 11, 27.

Xiao S, and Yu PH. (2009). A fluorometric high-performance liquid chromatography procedure for simultaneous determination of methylamine and aminoacetone in blood and tissues. Anal Biochem 384, 20–26.

Yu L, Liu P, Wang YL, et al. (2015). Profiling of aldehyde-containing compounds by stable isotope labelling-assisted mass spectrometry analysis. Analyst 140, 5276–5286.

Yuan D, Ma B, Yang JY, et al. (2009). Anti-inflammatory effects of rhynchophylline and isorhynchophylline in mouse N9 microglial cells and the molecular mechanism. Int Immunopharmacol 9, 1549–1554.

Yun H, Hou L, Song M, et al. (2012). Genomics and Traditional Chinese Medicine: A new driver for novel molecular-targeted personalized medicine? Curr Pharmacogenomics Person Med 10, 16–21.

Zhang HW, Tong J, Zhou G, Jia H, and Jiang JY. (2012). Tianma Gouteng Yin Formula for treating primary hypertension. Cochrane Database Syst Rev 6, CD008166.

Zhou R, Tseng CL, Huan T, and Li L. (2014). IsoMS: Automated processing of LC-MS data generated by a chemical isotope labeling metabolomics platform. Anal Chem 86, 4675–4679.

Address correspondence to:
Liang Li, PhD
Department of Chemistry
University of Alberta
Chemistry Centre W3-39
Edmonton
Alberta T6G2G2
Canada

E-mail: liang.li@ualberta.ca

and

Chun Wai Chan, PhD
School of Chinese Medicine
The Chinese University of Hong Kong
Shatin
New Territories
Hong Kong

E-mail: fcwchan@cuhk.edu.hk

Abbreviations Used

AGE = advanced glycation endproduct
CBF = cerebral blood flow
CCA = common carotid artery
CIL = chemical isotope labeling
CSF = cerebrospinal fluid
ECA = external cerebral artery
FTICR = Fourier transform ion cyclotron resonance
GE = *Gastrodia elata*
GS = glutamine synthetase
GUW = *Gastrodia elata* and *Uncaria rhynchophylla* water extract
H&E = hematoxylin and eosin
ICA = internal cerebral artery
LC-MS = liquid chromatography–mass spectrometry
LC-UV = liquid chromatography-ultraviolet
L-NMMA = L-N-monomethylarginine
MCAO = middle cerebral artery occlusion
MCID = MyCompoundID
OGD = oxygen–glucose deprivation
OPLS-DA = orthogonal partial least squares discriminant analysis
PBS = phosphate-buffered saline
PCA = principal component analysis
ROS = reactive oxygen species
RT = retention time
SD = standard deviation
TCM = Traditional Chinese Medicine
TTC = triphenyltetrazolium chloride
UR = *Uncaria rhynchophylla*